ACS OMEGA

http://pubs.acs.org/journal/acsodf

Article

Synthesis, Antitumor Activity, and *In Silico* Drug Design of New Thieno[2,3-*d*]Pyrimidine-4-One Derivatives as Nonclassical Lipophilic Dihydrofolate Reductase Inhibitors

Ola A. Abdelaziz, Walaa M. El Husseiny,* Khalid B. Selim, and Hassan M. Eisa

Cite This: *ACS Omega* 2022, 7, 45455−45468

Read Online

ACCESS | Metrics & More | Article Recommendations | Supporting Information

ABSTRACT: Synthesis of a new series of 20 compounds bearing the thieno[2,3-*d*]pyrimidine-4-one scaffold was achieved. The inhibitory activity of these compounds was performed over 60 cell lines of human tumor at single and five dose concentrations. Compounds **20**, **22**, and **23** exhibited potent growth inhibitions toward the majority of the tested NCI 60 cell lines. Compounds **20** and **23** were the most active compounds with (MG-MID) TGI, GI_{50}, and LC_{50} values of 16.2, 3.3, 50.1 and 67.7, 6.6, 100, respectively. Also, both compounds showed 7- and 4-fold better activity, respectively, than the standard antitumor agent 5-fluorouracil. Therefore, compounds **20** and **23** were selected to measure their ability to inhibit the dihydrofolate reductase enzyme (DHFR) in comparison to methotrexate (MTX) as a reference drug. Compound **20** was a more potent inhibitor of DHFR (IC_{50} = 0.20 μM) than MTX (IC_{50} = 0.22 μM). Molecular modeling studies were performed in the DHFR active site, and it showed compatibility with the results obtained from biological studies. Finally, the results showed that compound **20** is a strong antitumor agent and potent inhibitor of DHFR. In addition, this compound induced cell-cycle arrest in SNB-75 cells in the G2/M phase and the apoptosis process in the Pre-G phase. Compound **20** also increased the level of both caspases-3 and 9 by 11.8- and 50.3-fold, respectively.

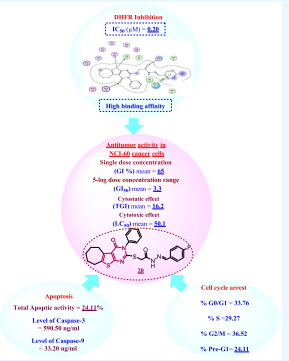

1. INTRODUCTION

Currently, cancer is the leading cause of fatality worldwide. The dihydrofolate reductase (DHFR) enzymatic pathway has been a significant goal in cancer therapy because DHFR is essential for reducing dihydrofolate into tetrahydrofolate[1] to afford one-carbon moieties for the synthesis of new thymidylate and purine nucleotides. Therefore, the inhibition of the DHFR enzyme leads to cancer cell death.[2]

Many thieno[2,3-*d*]pyrimidines have been reported as potent nonclassical lipophilic DHFR inhibitors.[3,4] Binding of thieno[2,3-*d*]pyrimidines to the DHFR enzyme is compared to folic acid binding; it is in the "flipped" mode where the sulfur of the thiophene pharmacophore was found to be able to mimic the 4-amino of methotrexate (MTX).[3,5,6]

Thieno[2,3-*d*]pyrimidine moieties are characterized by selectively targeting the tumor cells instead of the host normal cells because they target folate receptors (FRs), which are highly expressed in cancer cells, rather than target reduced folate carriers (RFCs), which are expressed in normal cells (Figure 1).[3,7]

As shown in Figure 2, reported structural features of thieno[2,3-*d*]pyrimidines as DHFR inhibitors showed that the nitrogen atom at position 1 and the NH_2 group at position 2 are essential for the formation of a salt bridge with the key amino acid Glu30.[8] In addition, the oxygen atom at position 4 is crucial for forming a hydrogen bond with Val115, Ile7, and Tyr121 amino acids.[3] Also, elongation of R_2 at position 6 by

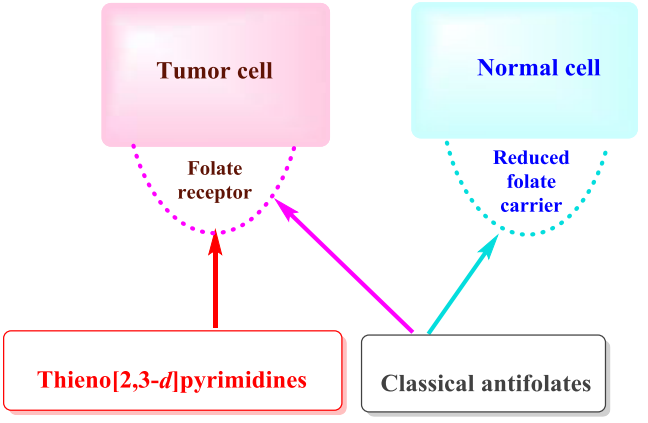

Figure 1. Tumor-targeting technique of thieno[2,3-*d*]pyrimidines.

replacing the methyl group with an ethyl group increases the potency against DHFR through increasing the lipophilicity of these inhibitors, which can facilitate passive diffusion.[6]

Received: September 20, 2022
Accepted: November 23, 2022
Published: December 2, 2022

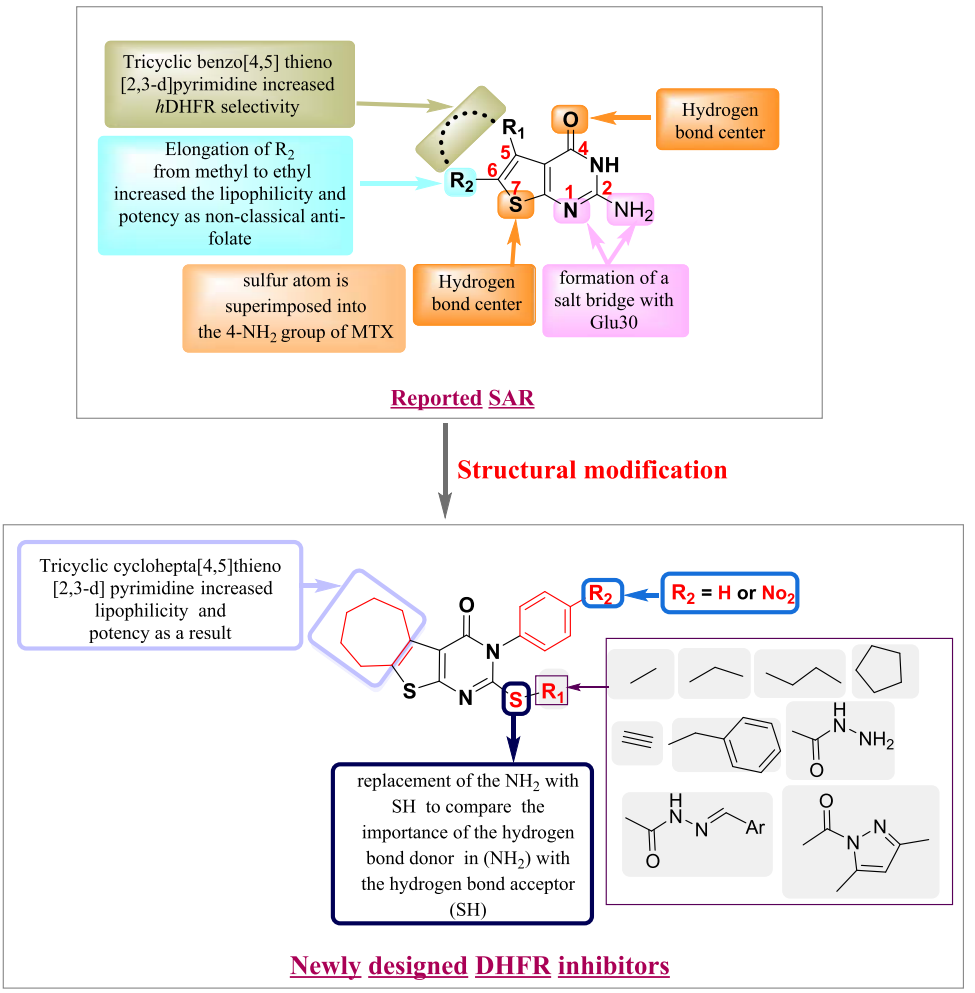

Figure 2. Design of new thieno[2,3-*d*]pyrimidine analogues as DHFR inhibitors.

Moreover, the presence of tricyclic benzo[4,5]thieno[2,3-*d*]pyrimidine-4-one was found to be more selective for human DHFR (*h*DHFR) in comparison to MTX. This selectivity is due to the presence of the sulfur atom at position 7, which is superimposed onto the MTX 4-NH_2 group.[3] Besides, it forms intermolecular H-bonds with Ile7 and Val115 amino acids through its carbonyl group and Tyr121 amino acid through its hydroxyl group.[8] Since the size of the sulfur atom is smaller than the size of carbon atoms and larger than the size of the nitrogen atom, the thiophene moiety, present in benzo[4,5]-thieno[2,3-*d*]pyrimidines, is used to mimic the activity of the larger quinazoline ring and the smaller pyrrole ring of MTX and pemetrexed (PMX), respectively.[6]

The aim of this work is to design new thieno[2,3-*d*]pyrimidine analogues accompanied by manipulation in their structures to evaluate their inhibitory effects toward DHFR activity. Moreover, *in vitro* cytotoxic activity against complete NCI 60 cell-line panels was evaluated, and the highest active compounds were selected to test their *h*DHFR inhibitory effect. Apoptotic and cell-cycle arrest analyses against the SNB-75 cell line were performed as well as the role of caspase-3 and caspase-9 in the signaling pathway of DHFR inhibitor-induced apoptosis was determined.

2. RESULTS AND DISCUSSION

2.1. Chemistry. Target compounds' synthesis was achieved through two schemes, Scheme 1 (for synthesis of compounds **7**−**16**) and Scheme 2 (for synthesis of compounds **17**−**24**). In Scheme 1, compound **2** was synthesized according to the Gewald reaction[9] through the interaction of cycloheptanone (**1**), ethyl cyanoacetate, and elemental sulfur in absolute ethanol using triethylamine (TEA) as a base catalyst. Reaction of ethyl carboxylate **2** with aryl isothiocyanates (R = H or NO_2) at room temperature using pyridine or THF as the solvent, respectively, gave thiourea derivatives **3** and **4**. Confirmation of structure **4** was done using ^{1}H NMR, in which two additional NH signals at 8.07 and 12.58 ppm appeared. Moreover, the presence of the aromatic ring was detected by the proton signals at 7.54−8.07 ppm. In the IR spectra, there was a (C═S) band at 853 and 1206 cm^{-1}, an (NO_2) band at 1342−1509 cm^{-1}, and a band at 3190 cm^{-1} characteristic to (NH), while the characteristic bands for the (NH_2) group at 3322 and 3465 cm^{-1} disappeared.

The synthesis of pyrimidin-4-ones **5** and **6** was performed through the cyclization of carbothioamides **3** and **4** in an aqueous potassium hydroxide solution.[10] The structure of the target compounds was confirmed in ^{1}H NMR spectra by the disappearance of the NH protons and the appearance of a new (SH) proton at 1.24−1.27 ppm.[11]

https://doi.org/10.1021/acsomega.2c06078
ACS Omega 2022, 7, 45455−45468

Scheme 1. Reagents and Conditions: (a) Ethyl 2-Cyanoacetate, Sulfur, Et_3N, rt; (b) Ar-SCN, Pyridine or THF, rt; (c) KOH/H_2O, 100 °C; (d) R−X, Acetone, K_2CO_3, 50 °C or rt; (e) R−X, DMF, K_2CO_3, rt

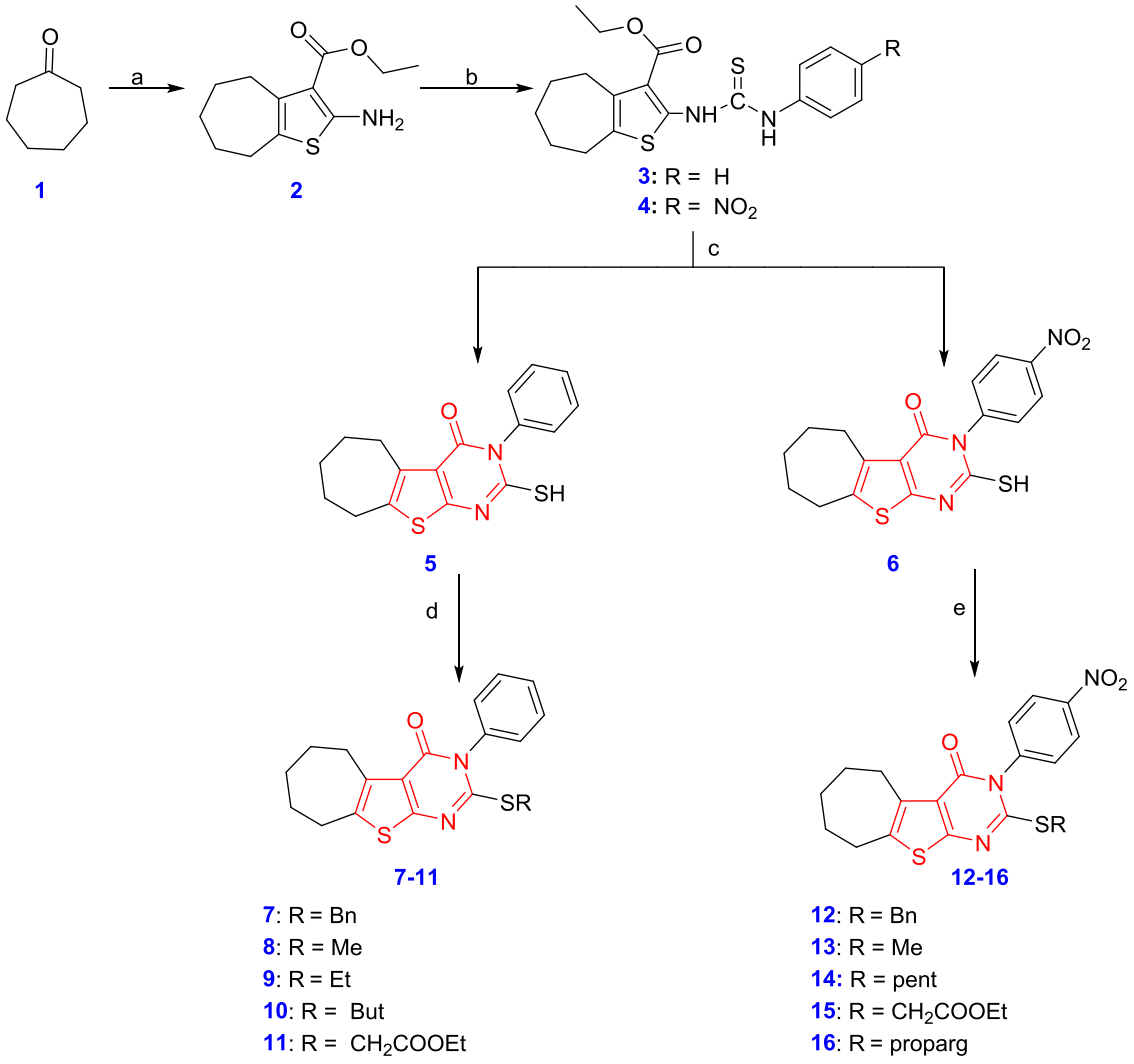

Two forms of tautomers, thiol and thione, could be expected from the cyclization of compounds **3** and **4**, under basic conditions.[12,13] From the NMR spectra, only the thiol tautomer of **5** and **6** was detected due to the presence of the (SH) proton at 1.27 ppm and the (C−SH) carbon at 147.8 ppm (Figure 3).

S-Alkylation of pyrimidin-4-one **5** was carried out through the reaction with several alkyl halides in acetone using K_2CO_3 as a base under reflux to prepare 2-(substituted thio)pyrimidin-4-ones **7**−**10**.[14] The formation of the ester derivative **11** was found to be temperature dependent as it was obtained at room temperature instead of under a refluxing condition. The ^{1}H NMR spectrum of compound **7** confirms its structure by the appearance of two benzylic protons at 4.37 ppm and the aromatic protons at 7.29−7.52 ppm. Also, ^{1}H NMR spectra of compounds **8**−**10** showed the presence of the signals of aliphatic protons at 0.84−3.02 ppm. Compound **11** showed triplet signals in its ^{1}H NMR spectrum at 1.22 ppm, singlet signals at 3.91 ppm, and quartet signals at 4.12 ppm attributed to $-OCH_2CH_3$, $-SCH_2$, and $-OCH_2CH_3$ protons, respectively. The signals of these groups in the ^{13}C NMR spectrum were detected at 14.65, 34.83, and 61.52 ppm, respectively.

To prepare 2-(substituted thio)pyrimidin-4-ones **12-1**, *S*-alkylation of pyrimidin-4-one **6** was performed by reacting with several alkyl halides in DMF using K_2CO_3 as the base, stirring at room temperature.[15,16] Confirmation of structure **12** was done using the ^{1}H NMR spectrum by the presence of the two benzylic protons at 4.39 ppm and the aromatic protons at 7.50−8.39 ppm. The structures of compounds **13** and **14** were detected in ^{1}H NMR spectra by additional singlet protons at 3.85 ppm and multiplet protons in the range of 1.45−1.89 ppm, attributed to methyl and cyclopentyl groups, respectively. For compound **15**, ester group signals were observed in the ^{1}H NMR spectrum at 1.22 ($-OCH_2CH_3$) and 4.12 ($-OCH_2CH_3$) ppm, in addition to singlet ($-SCH_2$) protons at 3.96 ppm. The IR spectra also showed the characteristic carbonyl ester band at 1733 cm^{-1}. Singlet signals at 3.22 and 3.95 ppm attributed to the propargaylic proton and $-SCH_2$ protons, respectively, were observed in the ^{1}H NMR spectrum of compound **16**. The same groups' signals were recorded in the ^{13}C NMR spectrum at 74.79, 79.35, and 21.13 ppm.

As shown in Scheme 2, acetohydrazide **17** was prepared by stirring the ester derivative **11** with hydrazine hydrate in absolute ethanol at room temperature for 48 h.[17] The ^{1}H NMR spectrum of acetohydrazide **17** showed new signals

https://doi.org/10.1021/acsomega.2c06078
ACS Omega 2022, 7, 45455−45468

Scheme 2. Reagents and Conditions: (a) NH_2NH_2, Ethanol, rt; (b) Ar-CHO, EtOH, 90 °C; (c) Acetylacetone, EtOH, 90 °C

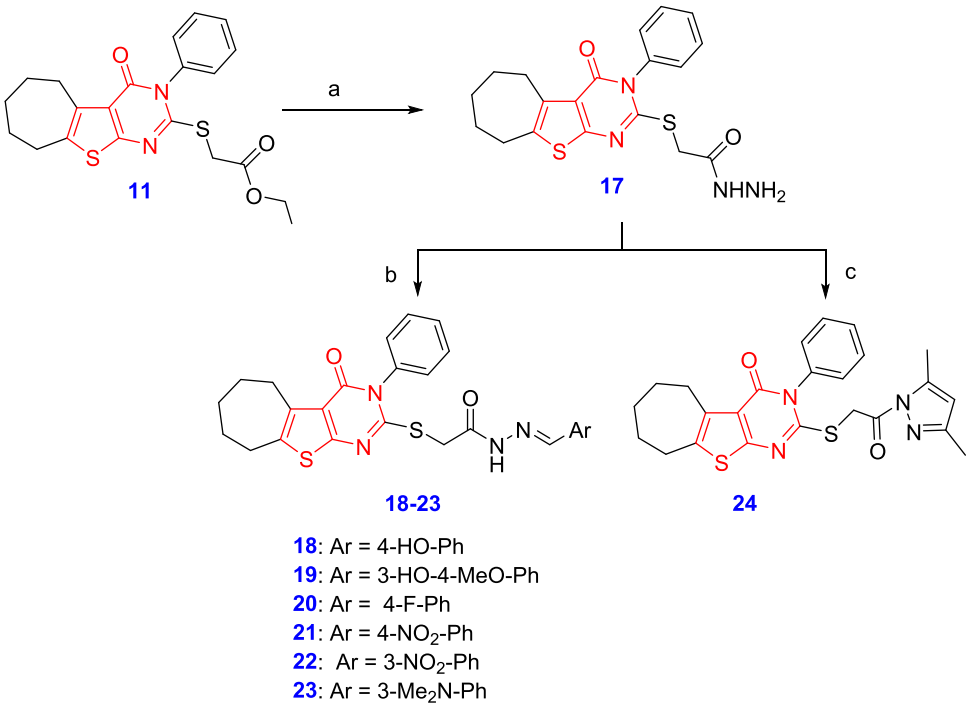

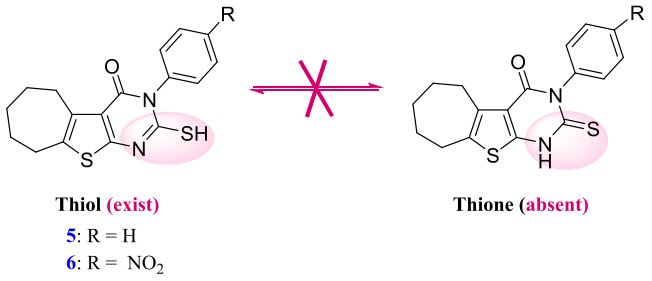

Figure 3. Possibilities of thiol-thione tautomerism.

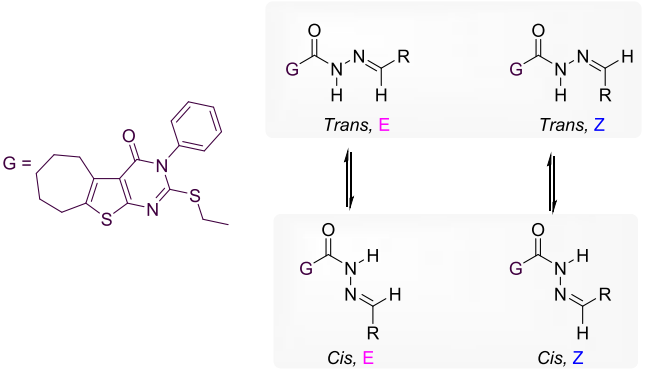

Figure 4. Geometrical isomers and conformers of Schiff bases **18**−**23**.

appeared at 4.26 and 9.29 ppm, respectively, attributed to the protons of NH_2 and NH of the hydrazide structure along with the disappearance of the signals of the ethoxy group. Also, the IR spectrum showed the appearance of the carbonyl hydrazide band at 1645 cm^{-1} and the disappearance of the carbonyl easter band at 1736 cm^{-1}.

Schiff bases **18**−**23** were synthesized through the reaction of different aromatic aldehydes with acetohydrazide **17** using ethanol as a solvent.[16] The ^{1}H NMR spectra of these compounds showed additional signals in the range from 6.72 to 8.28 ppm owing to the aromatic ring and singlet signals in the range from 7.87 to 8.53 ppm owing to the ylidenic proton HC=N.

It was observed that two signal sets of $-SCH_2$, −NH, and −N=CH groups of these compounds were observed in their ^{1}H NMR spectra as *trans* and *cis* conformers. In the *cis* conformer, −NH and −N=CH protons' lines appeared upfield, while in the *trans* conformer, the lines of the protons of the same groups appeared downfield (Figure 4).[18]

The Knorr pyrazole reaction was utilized for the synthesis of pyrazole **24** through the interaction of acetohydrazide **17** with acetylacetone in absolute ethanol.[19] No signals belonging to NH or NH_2 protons were displayed for this compound in its ^{1}H NMR spectrum; instead, new singlet signals appeared at 6.39, 1.7, and 1.99 ppm, attributed to CH−pyrazole and the two CH_3 groups, respectively.

2.2. Biology. *2.2.1. Cytotoxicity Screening.* For screening the antitumor activity, a screening panel assay for *in vitro* disease-oriented human cells was run at the National Cancer Institute (NCI). It was dependent on the usage of a single dose of tested compounds (10 μM) in the complete NCI 60 cell-line panel assay that contains cancer subpanels, namely, breast, renal, prostate, melanoma, colon, CNS, non-small-cell lung, ovarian, and leukemia cancer cells.[20,21] The capability of the tested compounds to produce inhibition of cancer growth was represented by the percentage growth inhibition (GI %) (Table 1).

In the current investigation, the antitumor activity of a broad spectrum was observed by the majority of the tested compounds **4**, **12**−**23**. It was found that different antitumor activities were related to different structural characteristics. Generation of different substituted thio derivatives was aimed to discover their structure−activity relationship (SAR). The substituted thio derivatives **7**−**11** showed low potency *versus* tumor cell lines and were regarded as the least effective

https://doi.org/10.1021/acsomega.2c06078
ACS Omega 2022, 7, 45455−45468

Table 1. (GI %) Percentage Growth Inhibition Resulting from Compounds' Concentration of 10 μM (4, 12−23) of Subpanel Tumor Cell Lines[a]

subpanel tumor cell lines (sample conc. = 10 μM)	% growth inhibition (GI %)										
	4	**12**	**13**	**14**	**15**	**16**	**18**	**19**	**20**	**22**	**23**
leukemia											
CCRF-CEM	**36**	7	10	7	11	12	**30**	22	**54**	24	**30**
HL-60(TB)	**30**	3	8	13	12	9	–	22	–	–	14
RPMI-8226	**53**	7	2	–	9	16	7	9	**34**	**44**	**34**
SR	**38**	15	22	11	24	12	16	17	**89**	**62**	**78**
non-small-cell lung cancer											
HOP-62	–	27	18	–	**53**	7	–	–	**80**	**47**	**79**
HOP-92	**100**	6	8	18	20	13	–	–	18	27	**50**
A549/ATCC	15	19	–	8	**34**	6	9	2	**91**	**73**	**94**
EKVX	21	15		19	18	13	13	21	20	**30**	**53**
NCI-H460	**31**	26	15	10	**52**	6	4	–	**90**	**81**	**99**
NCI-H522	**42**	19	20	15	**32**	20	20	24	**56**	**47**	**79**
NCI-H322M	**30**	12	15	10	23	11	–	3	**33**	21	**56**
NCI-H23	**31**	**46**	1	1	26	5	3	2	**63**	**46**	**71**
colon cancer											
HCC-2998	3	–	–	6	18	–	–	–	–	3	**61**
HCT-116	**30**	16	-	9	**49**	23	3	3	**126**	**96**	**93**
COLO 205	–	1	–	2	18	–	–	–	**62**	11	**67**
HCT-15	**33**	6	3	6	15	8	3	15	**52**	**47**	**57**
HT29	–	8	2	–	22	2	–	–	**74**	**68**	**55**
KM12	28	–	6	13	11	9	–	–	**58**	**53**	**62**
SW-620	1	5	9	1	19	6	–	–	**47**	**48**	**73**
CNS cancer											
SF-268	11	2	12	4	29	10	–	–	**92**	**56**	**63**
SF-295	13	**32**	6	2	23	11	7	7	**84**	24	**81**
SF-539	8	5	2	–	25	–	–	–	**139**	**99**	**66**
SNB-75	14	15	18	3	**89**	7	–	–	**165**	**94**	**102**
U251	23	16	19	18	**47**	6	–	5	**93**	**51**	**95**
melanoma											
LOX IMVI	16	6	8	3	21	21	**40**	16	**63**	24	**63**
MALME-3	28	9	1	4	23	5	–	28	**89**	26	**65**
M14	7	6	4	6	25	15	–	7	**49**	29	**54**
MDA-MB-435	12	3	1	–	23	10	–	12	**40**	28	**67**
SK-MEL-2	**34**	–	–	–	10	3	3	**34**	9	10	22
SK-MEL-28	15	–	–	–	16	–	–	15	**52**	26	**53**
SK-MEL-5	**57**	4	3	5	12	9	9	–	**50**	**33**	**54**
UACC-257	**30**	9	6	10	11	3	–	30	26	**34**	**36**
UACC-62	**52**	13	15	8	26	8	45	**52**	17	**35**	**92**
ovarian cancer											
786-0	7	5	7	7	29	–	–	–	**36**	20	**55**
A498	**50**	20	9	6	15	1	**45**		11	17	**65**
ACHN	15	**33**	16	15	**48**	10	3	17	**74**	20	**75**
CAKI-1	21	29	8	–	**49**	**32**	14	24	**113**	**41**	**91**
RXF 393	16	16	27	13	**34**		6	–	**95**	**39**	**106**
SN12C	**45**	12	**34**	28	16	12	23	26	**84**	**34**	**44**
prostate cancer											
PC-3	**57**	**55**	17	10	27	25	6	14	**55**	**62**	**123**
DU-145	9	1	5	4	**61**	2	–	–	**113**	**101**	77
breast cancer											
MCF7	**30**	14	11	15	27	21	1	17	**74**	**55**	**65**
MDA-MB-231/ATCC	21	25	10	7	**50**	25	9	24	**126**	**49**	**57**
HS 578T	9	18	–	–	**61**	2	–	–	**113**	**101**	77
BT-549	6	–	–	–	3	–	2	11	**52**	**62**	29
T-47D	12	**61**	15	12	24	19	17	17	**84**	**36**	**39**
MDA-MB-468	29	17	3	–	**44**	–	–	–	**103**	**81**	**74**
MG-MID	25	11	8	6	28	9	2	5	**65**	**44**	**62**

[a]– represents GI ≤ 10%. Bold numbers represent the high % GI. Underlined numbers represent GI ≥100% "Lethal activity". MG-MID represents full-panel mean-graph midpoint.

https://doi.org/10.1021/acsomega.2c06078
ACS Omega 2022, 7, 45455−45468

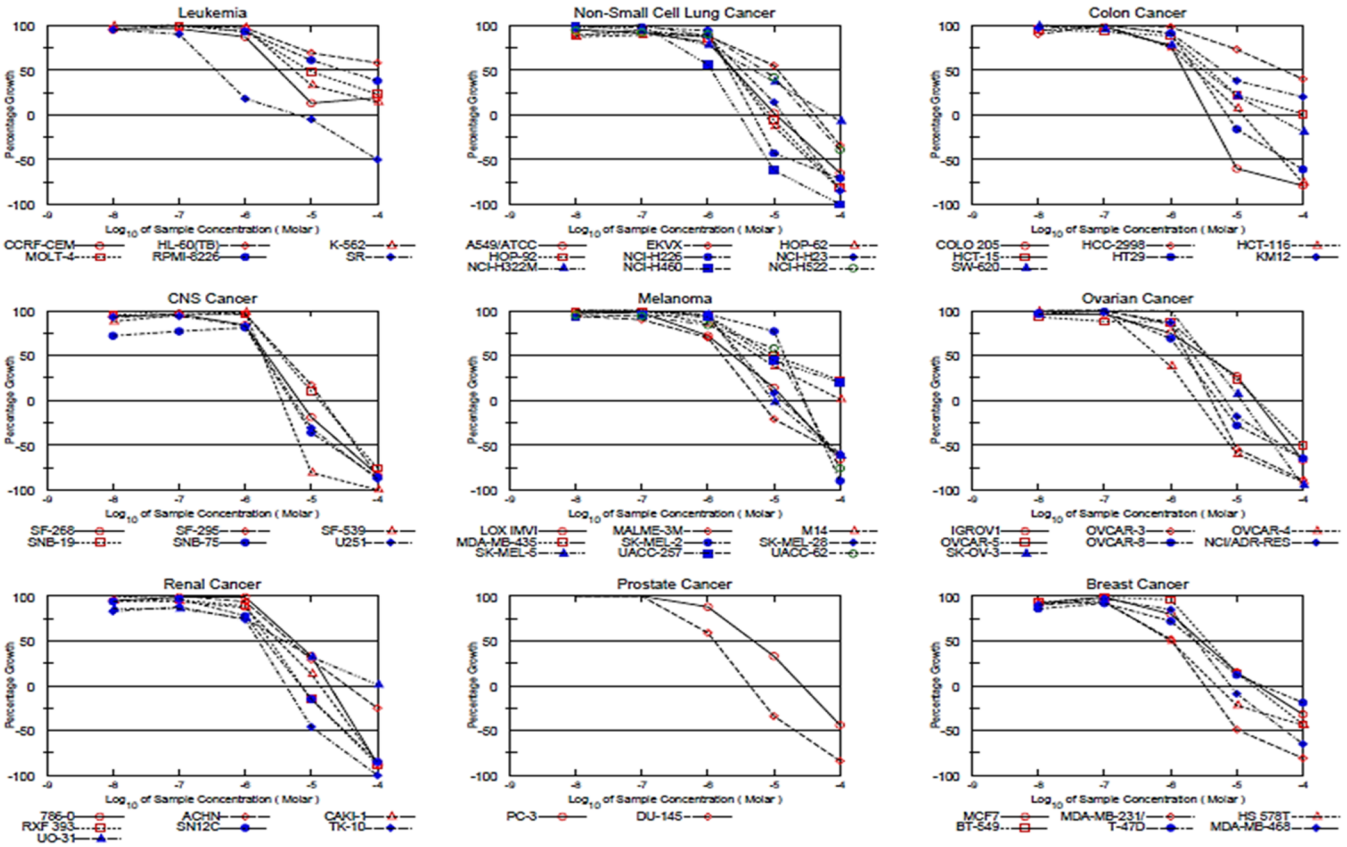

Figure 5. Dose−response curve of compound **20** in all cancer lines.

participants. However, introduction of an electron-withdrawing nitro group as in derivatives **12**−**16** increased the antitumor activities. Incorporation of unsaturation as in derivatives **12** and **16** showed potent antitumor activities compared to saturated derivatives **13**−**15**. Different derivatives of Schiff bases were prepared to discover their SAR. The introduction of a hydroxyl group produced Schiff base derivatives with a low antitumor activity such as **18** and **19**, suggesting that a hydrophilic group is not preferable. However, exchanging the hydrophilic group with a lipophilic one such as a dimethyl amino group and a fluorine atom resulted in potent compounds **23** and **20**, respectively.

NCI assay results revealed that many compounds showed high selectivity with potent growth inhibition. Compounds with high selectivity include compound **4**, which is obviously selective with GI % of about 100% against the cancer cell line of the non-small-cell lung, compounds **13** and **16** with GI % ranging from 32 to 34% against the renal cancer cell line, compound **18** showed selectivity against the melanoma cell line with GI % ranging from 40 to 45%, and compound **19** also showed GI % ranging from 30 to 34% against leukemia and melanoma cell lines. It is worthy to mention that compounds **20**, **22**, and **23** possessed the highest potency and also showed lethal activity against certain cancer cell lines. All of the tested cell lines were highly sensitive to compound **22** with very high GI % values.

Compounds **20** and **23** proved to be the best among all tested compounds, with GI % mean values of 65 and 62%, respectively. Therefore, both compounds passed the primary anticancer test at 10 μM concentration and were selected by NCI for conducting further assays at five concentrations (5-log dose range), which could better capture the potency of these compounds. Monitoring of GI_{50}, TGI, and LC_{50} as the three response parameters for each cell line was done (Figures 5−7).

As shown in Table 2, compound **20** was 7-fold more active than the standard 5-FU, with full-panel mean-graph midpoint (MG-MID) TGI, GI_{50}, and LC_{50} values of 16.2, 3.3, and 50.1, respectively. However, compound **23** was 4-fold more active than the standard drug, with MG-MID TGI, GI_{50}, and LC_{50} values of 67.7, 6.6, and 100, respectively.

2.2.2. Human Dihydrofolate Reductase (hDHFR) Inhibition Assay. Regarding the NCI results, compounds **20** and **23** were selected for the assay of *h*DHFR inhibition using MTX as a reference drug. It was observable that these compounds exhibited high inhibitory activity (IC_{50} = 0.20 and 0.28 μM, respectively), which was comparable to the inhibitory activity of MTX (IC_{50} = 0.22 μM). The results suggested that *h*DHFR inhibition might be responsible for the cytotoxic activity of the tested compounds (Table 3).

2.2.3. Analysis of Cell-Cycle Arrest. Previous assays showed that compound **20** has broad-spectrum activity that was remarkable against many tested cell lines of human cancer, especially against the SNB-75 cell line. Therefore, it was more investigated, relative to MTX, to explore its mechanism of action. Thus, measurement of DNA contents of the SNB-75 cell line was carried out depending on the flow cytometry technique in which the cell line was treated first with compound **20** for 24 h and propidium iodide was used for staining before measuring the DNA contents (Table 4 and Figure 8).

The cell proportion in the S phase after treating SNB-75 cells with compound **20** decreased to 29.72% when compared

https://doi.org/10.1021/acsomega.2c06078
ACS Omega 2022, 7, 45455−45468

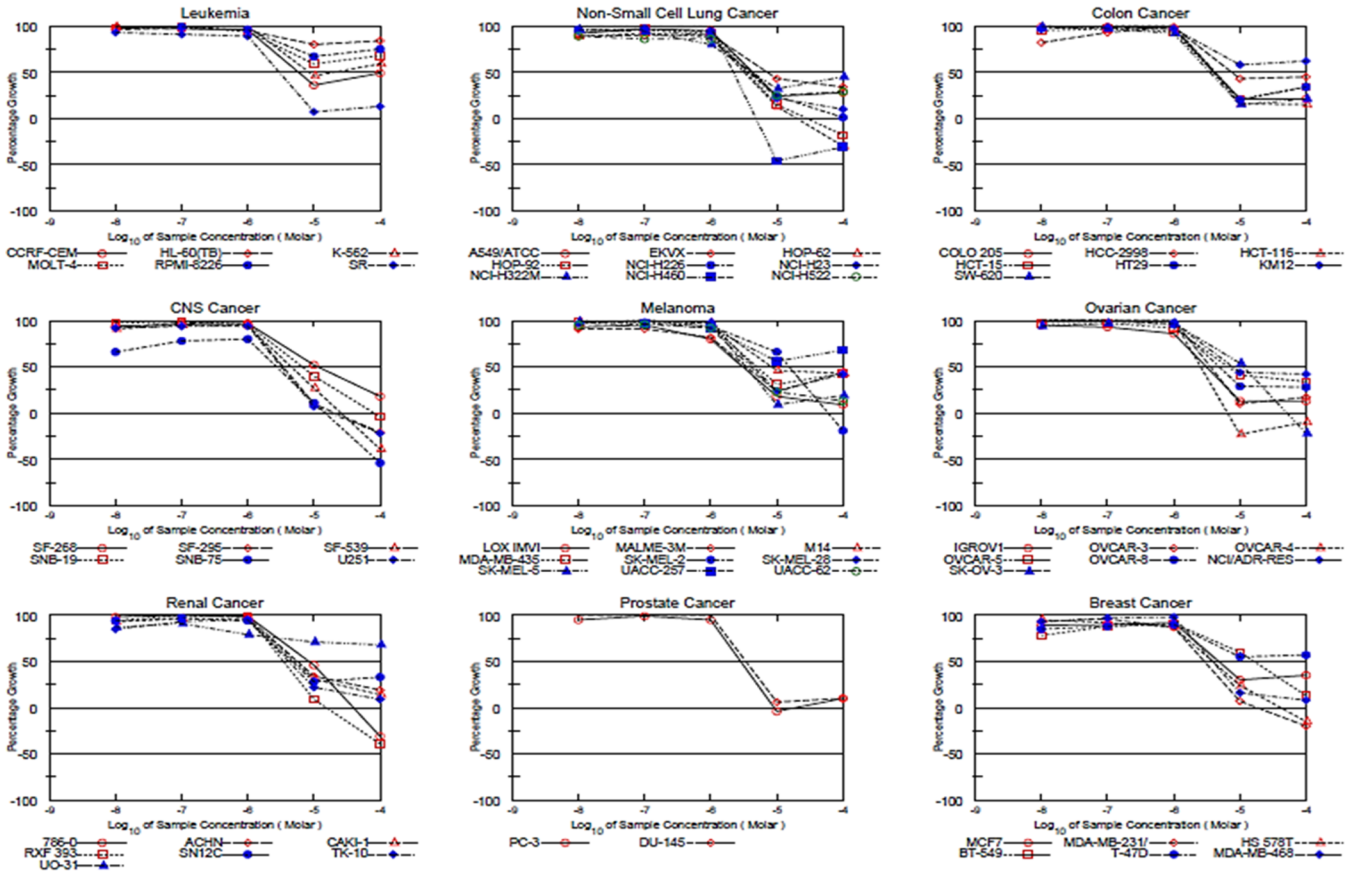

Figure 6. Dose−response curve of compound **23** in all cancer lines.

to the control cell (36.28%). In addition, there was an increase in the cell proportion up to 36.52% in the G2/M phase due to compound **20** in comparison to the control cell (5.48%). This indicates that the G2/M phase is the one in which cells were arrested. On the other hand, treatment with compound **20** leads to the pre-G1 population (24.11%), while that of the controlled cell is 1.38%, which indicates that compound **20** had a great influence on cell-cycle distribution and induced cytotoxicity as a result of cell-cycle arrest

2.2.4. Apoptotic Assay. Cells were treated with compound **20** and suspended in Annexin V-FITC and PI for 24 h. Annexin V-FITC and PI were used for detecting apoptosis and necrosis, respectively. The apoptotic cell population was increased in SNB-75-treated cells in comparison to the untreated cells. These results indicated that compound **20** induced apoptosis by 24.11% (Table 5 and Figure 9).

2.2.5. Detection of Protein Levels of Caspases-3 and 9. Determination of caspases-3 and caspase-9 levels is regarded as an essential method to detect the pathway involved in the process of apoptosis. The level of caspase-3 and caspase-9 in SNB-75 cells was measured after 24 h treatment of these cells with compound **20**. It was found that our compound increased the level of caspase-3 and caspase-9 by 11.8- and 50.3-fold, respectively, which is compatible with cell-cycle arrest analysis data (Table 6).

2.2.6. In Silico Study. According to the significant results of *h*DHFR inhibition activity, it was exciting to further study the docking of compounds **20**, **22**, and **23**, which had the highest DHFR inhibitory activity, into the binding site of *h*DHFR and explore the interaction of these compounds in the *h*DHFR pocket with its amino acids. Docking was done using molecular operating environment (MOE) software version 2014.09. The crystal structure of the DHFR complex with MTX (PDB code 1U72) was important to identify the 2D ligand interaction of DHFR and MTX. The pattern of binding between the DHFR receptor active site and MTX revealed the key amino acids of the *h*DHFR pocket through the trifurcated H-bonds that were built with the "catalytic triad" Ile7, Tyr121 and Val115 residues, and the pocket residues Glu30 and Asn64 form stable H-bonds[22] (Figure 10).

The 2D binding configuration shows that skeletons of our compounds are deeply inhumed inside the pocket, and a tortuous "L" structure was formed by those compounds through the bridge region, which enables them to interact with most of the key amino acids. They can interact with Asn64 through their amide linkers, with Val115 through their thiophene moieties, with Arg70 through their pyridine rings, and with Phe31 through their aromatic rings. Although they have the same structures, they have slightly different enzymatic activities as there is a specific pattern of configuration for each compound inside the pocket. Therefore, compound **20** has the ability to bind to the key pocket residue Tyr121 (Figure 11A), while compound **23** does not. The activity of **23** is reduced due to this binding, where the thiophene moiety is positioned away from Tyr121 (Figure 11B). For compound **22**, its nitro group at the *meta* position enables it to interact with most of the key amino acids such as Arg70 and Asn64. It can also bind to Phe31 through its aromatic ring. Its different configuration inside the pocket directs its thiophene ring away from both key

https://doi.org/10.1021/acsomega.2c06078
ACS Omega 2022, 7, 45455−45468

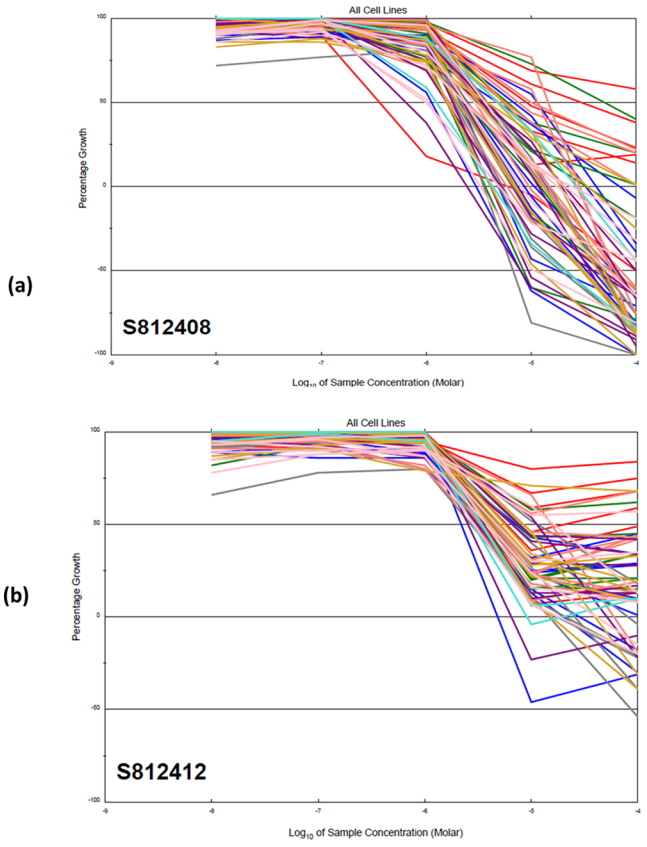

Figure 7. Dose−response graphs of the NCI 60 cell-line panel exposed to (a) compound **20** (NSC 812408) and (b) compound **23** (NSC 812412). The graph is coded with the color of the tissue origin: pink for breast cancer, turquoise for prostate cancer, gold for renal cancer, coral for the melanoma cell line, purple for ovarian cancer, green for colon cancer, gray for central nervous system cancer, blue for lung cancer, and red for the leukemia cell line.

Table 2. Mean Sensitivity of Compounds 20 and 23 across All Cell Lines

	full-panel mean-graph midpoint MG-MID (mM)		
compound	GI_{50}	TGI	LC_{50}
20	3.3	16.2	50.1
23	6.6	67.7	100
5-flourouracil (5-FU)	22.6	>100	>100

Table 3. *h*DHFR Inhibitory Activity of Compounds 20 and 23

compound	*h*DHFR inhibition IC_{50} (μM)
20	0.20
23	0.28
MTX	0.22

Table 4. Analysis of Compound 20 Cell-Cycle Arrest Using Flow Cytometry Relative to MTX

	analysis of cell-cycle arrest (%)			
	G0/G1	S	G2/M	pre-G1
20/SNB-75	33.76	29.72	36.52	24.11
MTX/SNB-75	29.36	26.81	43.83	27.38
control/SNB-75	58.24	36.28	5.48	1.38

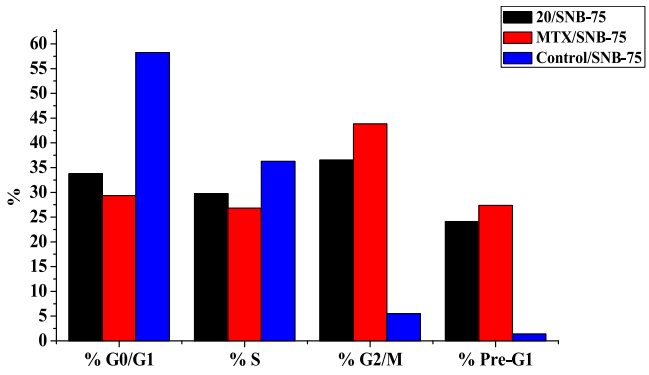

Figure 8. Cell-cycle distribution of the SNB-75 cell line by compound **20**.

Table 5. Apoptotic Activities of Compound 20

	apoptosis			
compounds	early	late	necrosis	total
20/SNB-75	8.49	13.43	2.19	24.11
MTX/SNB-75	6.78	18.08	2.52	27.38
control/SNB-75	0.73	0.28	0.37	1.38

amino acids yr121 and Val115. This binding shows why compound **22** has reduced activity (Figure 11C).

3. CONCLUSIONS

In this work, new thieno[2,3-*d*]pyrimidines **4**−**24** were synthetized and evaluated for their cytotoxic activity against complete NCI 60 cell-line panels. The target compounds **20**, **22**, and **23** are characterized by having the highest DHFR inhibitory activity. The docking studies that were carried out proved that these compounds are highly potent as DHFR inhibitors. Moreover, compound **20** induced Pre-G apoptosis and G2/M cell-cycle arrest in SNB-75 cells.

4. EXPERIMENTAL SECTION

4.1. Chemistry. The Stuart apparatus was used for recording of the melting points, and they were uncorrected. NMR spectra (^{1}H and ^{13}C) were recorded on Bruker 400 MHz and Joel 500M FT NMR spectrometers with tetramethyl silane (TMS) as the standard. (DMSO-d_6) and ($CDCl_3$) were the used solvents, and chemical shifts were obtained in δ (ppm) at the Unite of Nuclear Magnetic Resonance, Faculties of Science and Pharmacy, Mansoura University. Recording of mass spectra (MS) was done by the Hewlett Packard 5988 spectrometer (EI) in Al-Azhar University, Cairo, Egypt, and the spectrometer of Advion compact mass (ESI) in the Scientific laboratory of Nawah, Cairo, Egypt. IR spectra (KBr) (υ in cm^{-1}) were recorded at the Unit of Central Laboratory in the Pharmacy Faculty of Mansoura University using the IR spectrometer of Nicolet iS10FT. TLC was used for recording the reaction time using silica gel plates (60 F245E). Merk. Spot visualization was done using UV (366 nm). All of the chemicals used were from Aldrich, and they needed no further purification. Compounds **2**,[23] **3**,[24] and **5**[25] have been described elsewhere.

*4.1.1. Synthesis of Ethyl 2-[3-(4′-Nitrophenyl)-carbothioamido]-5,6,7,8-tetrahydro-3H-cyclohepta[b]-thiophene-3-carboxylate (**4**).* *p*-Nitrophenyl isothiocyanate (0.72 g, 4 mmol) was added to compound **2** solution (0.96 g, 4 mmol) in THF (10 mL). This mixture was stirred for 24 h at

https://doi.org/10.1021/acsomega.2c06078
ACS Omega 2022, 7, 45455−45468

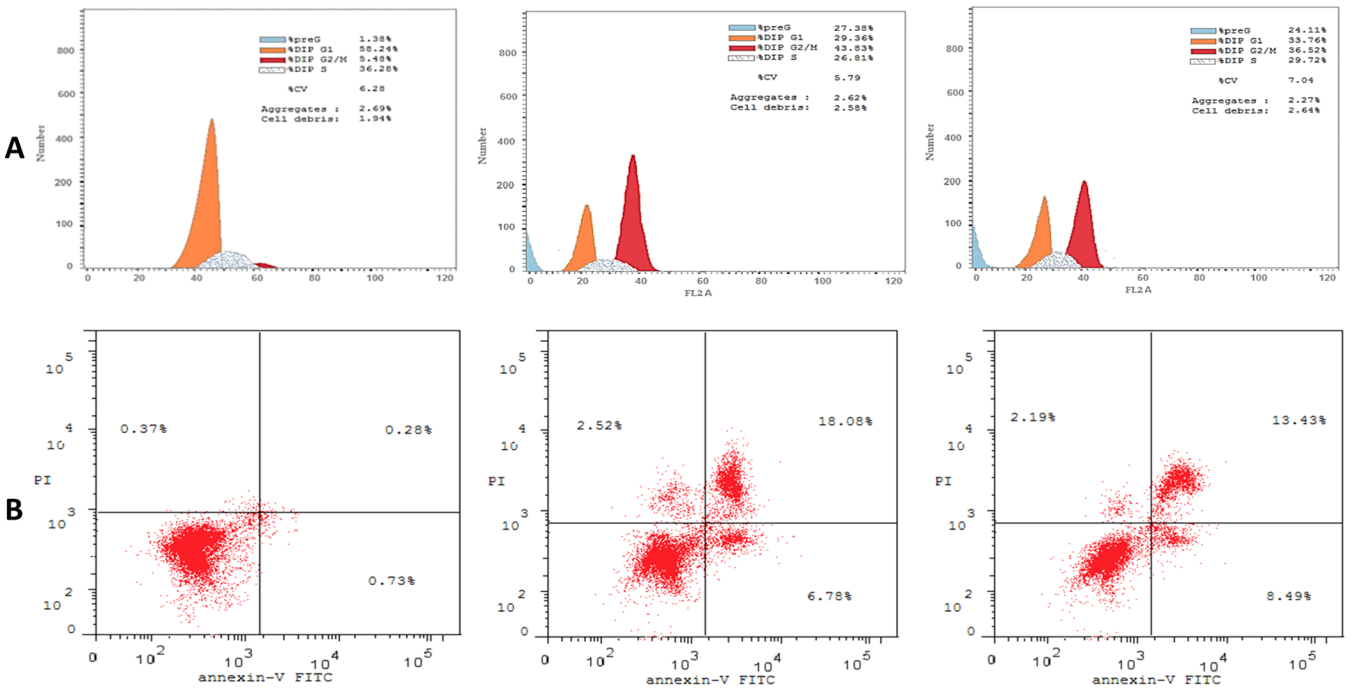

Figure 9. (A) SNB-75 cell line's cell-cycle distribution by compound **20**. (B) Apoptotic effect of compound **20** on the human SNB-75 cell line.

Table 6. Caspases-3 and Caspase-9 (ng/mL) Detection Assay

compound	caspase-3	caspase-9	caspase-3 fold	caspase-9 fold
20	590.5	33.2	11.8	50.3
control/MCF7	50	0.66		

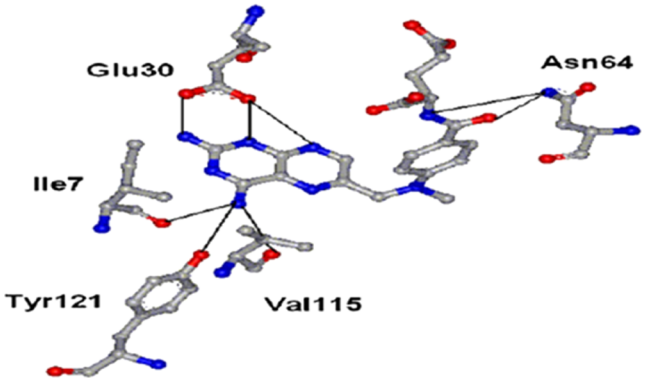

Figure 10. 2D ligand interaction of DHFR and MTX.

room temperature. After that, it was poured on crushed ice, followed by separation of the precipitated solid by filtration, washing with water, and recrystallization from EtOH, giving an orange solid; yield = 95%, melting point = 171−173 °C. IR (KBr, υ, cm^{-1}): 1342, 1509 (NO_2), 1546 (C═S), 1662 (C═O), 3190 (NH). ^{1}H NMR (400 MHz, $CDCl_3$): δ 1.31 (t, J = 7.1 Hz, 3H, $CH_2\underline{CH_3}$), 1.61 (m, 4H, $2CH_2$), 1.81 (m, 2H, CH_2), 2.71 (m, 2H, CH_2), 2.99 (m, 2H, CH_2) 4.24 (q, J = 7.1 Hz, 2H, $\underline{CH_2}CH_3$), 7.54 (d, J = 9.0 Hz, 2H, Ar-H), 8.07 (s, 1H, NH; D_2O exchangeable), 8.25 (d, J = 9.0 Hz, 2H, Ar-H), 12.58 (s, 1H, NH; D_2O exchangeable).

*4.1.2. Synthesis of 3-(4-Nitrophenyl)-2-sulfanyl-6,7,8,9-tetrahydro-3H-cyclohepta[4,5]thieno[2,3-d]pyrimidin-4-(5H)-one (**6**).* A solution of compound **4** (4.19 g, 10 mmol) in aqueous KOH (6%, 60 mL) was refluxed for 2 h and then concentrated. The concentrate was dissolved in water and neutralized with HCl (1 M). The precipitated solid was filtered, washed with water, dried, and recrystallized from EtOH to give a yellow solid; yield = 88%, melting point = 223−225 °C, IR (KBr, υ, cm^{-1}): 1345, 1520 (NO_2), 1648 (C═O), 3407 (NH). ^{1}H NMR (400 MHz, $CDCl_3$): δ 1.22 (s, 1H, SH), 1.67 (m, 4H, $2CH_2$), 1.84 (m, 2H, CH_2), 2.73 (m, 2H, CH_2), 3.13 (m, 2H, CH_2), 7.42 (d, J = 7.4 Hz, 2H, Ar-H). 8.37 (d, J = 7.4 Hz, 2H, Ar-H). ^{13}C NMR (100 MHz, $CDCl_3$): δ 27.25, 27.57, 27.70, 29.39, 32.25, 117.69, 124.57, 124.99, 130.17, 130.23, 138.28, 147.80.

*4.1.3. General Procedure for the Synthesis of 2-(Alkylthio)-3-phenyl-6,7,8,9-tetrahydro-3H-cyclohepta[4,5]-thieno[2,3-d]pyrimidin-4-(5H)-ones (**7**−**11**).* The appropriate alkyl halide (1.5 mmol) was added to a mixture of K_2CO_3 (0.18 g, 1 mmol) and compound **5** (0.32 g, 1 mmol) in acetone (5 mL). It was refluxed at 60 °C for 8 h and was TLC-monitored precisely. After reaction accomplishment, acetone was evaporated under a vacuum, and the obtained residue was recrystallized from EtOH.

*4.1.3.1. 2-(Benzylthio)-3-phenyl-6,7,8,9-tetrahydro-3H-cyclohepta[4,5]thieno[2,3-d]pyrimidin-4-(5H)-one (**7**).* Using benzyl chloride (0.19 g, 1.5 mmol) as the alkyl halide yielded a white solid; yield = 74%, melting point = 237−239 °C. ^{1}H NMR (400 MHz, $CDCl_3$): δ 1.66 (m, 4H, $2CH_2$), 1.89 (m, 2H, CH_2), 2.87 (m, 2H, CH_2), 3.30 (m, 2H, CH_2), 4.37 (s, 2H, $\underline{CH_2}$−S), 7.29 (m, 5H, Ar-H), 7.38 (d, J = 7.8 Hz, 2H, Ar-H), 7.52 (d, J = 7.8 Hz, 3H, Ar-H).

*4.1.3.2. 2-(Methylthio)-3-phenyl-6,7,8,9-tetrahydro-3H-cyclohepta[4,5]thieno[2,3-d]pyrimidin-4-(5H)-one (**8**).* Using methyl iodide (0.21 g, 1.5 mmol) as the alkyl halide yielded a white solid; yield = 70%, melting point = 187−189 °C, IR (KBr, υ, cm^{-1}): 1509 (olefinic C═C), 1668 (C═O). ^{1}H NMR (400 MHz, DMSO-d_6): δ 1.60 (m, 4H, $2CH_2$), 1.85 (m, 2H, CH_2), 2.42 (s, 3H, CH_3), 2.84 (m, 2H, CH_2), 3.18 (m,

https://doi.org/10.1021/acsomega.2c06078
ACS Omega 2022, 7, 45455−45468

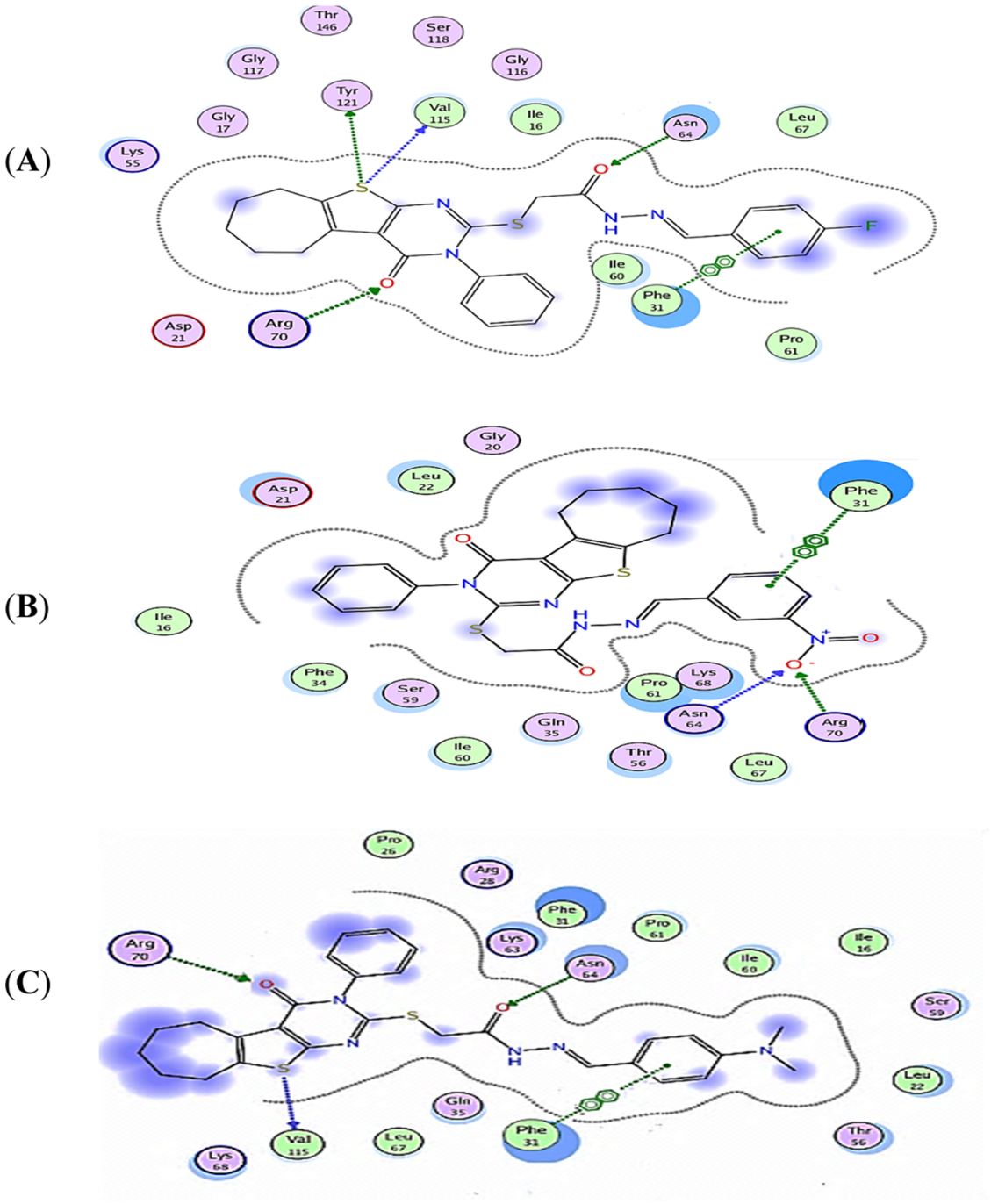

Figure 11. (A) 2D binding configuration of DHFR and compound **20**. (B) 2D binding configuration of DHFR and compound **22**. (C) 2D binding configuration of DHFR and compound **23**.

2H, CH_2), 7.38 (d, J = 6.7 Hz, 2H, Ar-H). 7.52 (d, J = 6.7 Hz, 3H, Ar-H).

*4.1.3.3. 2-(Ethylthio)-3-phenyl-6,7,8,9-tetrahydro-3H-cyclohepta[4,5]thieno[2,3-d]pyrimidin-4-(5H)-one (**9**).* Using ethyl iodide (0.22 g, 1.5 mmol) as the alkyl halide yielded a white solid; yield = 72%, melting point = 157−159 °C, IR (KBr, υ, cm^{-1}): 1509 (C═C), 1683 (C═O). ^{1}H NMR (400 MHz, $CDCl_3$): δ 1.23 (t, J = 7.4 Hz, 3H, S-$CH_2\underline{CH_3}$), 1.61 (m, 4H, $2CH_2$), 1.80 (m, 2H, CH_2), 2.76 (m, 2H, CH_2), 3.02 (2H, q, J = 7.4 Hz, S−$\underline{CH_2}CH_3$), 3.2 (m, 2H, CH_2), 7.24 (d, J = 6.7 Hz, 2H, Ar-H). 7.50 (d, J = 6.7 Hz, 3H, Ar-H).

*4.1.3.4. 2-(Butylthio)-3-phenyl-6,7,8,9-tetrahydro-3H-cyclohepta[4,5]thieno[2,3-d]pyrimidin-4-(5H)-one (**10**).* Using butyl iodide (0.28 g, 1.5 mmol) as the alkyl halide yielded a white solid; yield = 76%, melting point = 170−172 °C. ^{1}H NMR (400 MHz, $CDCl_3$): δ 0.84 (t, J = 7.3 Hz, 3H, $CH_2CH_2CH_2\underline{CH_3}$), 1.32 (dq, J = 7.3−14.5 Hz, 2H, $CH_2CH_2\underline{CH_2}CH_3$), 1.53 (m, J = 7.3 Hz, 2H, $CH_2\underline{CH_2}CH_2CH_3$), 1.62 (m, 4H, $2CH_2$), 1.80 (m, 2H, CH_2), 2.76 (m, 2H, CH_2), 3.02 (m, J = 7.3 Hz, 2H, $\underline{CH_2}CH_2CH_2CH_3$), 3.2 (m, 2H, CH_2), 7.24 (d, J = 6.3 Hz, 2H, Ar-H), 7.50 (d, J = 6.3 Hz, 3H, Ar-H).

4.1.3.5. Ethyl 2-[(4-Oxo-3-phenyl-6,7,8,9-tetrahydro-3H-cyclohepta[4,5]thieno[2,3-d]pyrimidin-5H-2-yl)thio]acetate (11). Using ethyl chloroacetate (0.18 g, 1.5 mmol) as the alkyl

https://doi.org/10.1021/acsomega.2c06078
ACS Omega 2022, 7, 45455−45468

halide yielded a white solid; yield = 88%, melting point = 188−190 °C, IR (KBr, υ, cm^{-1}): 1517 (C═C), 1680 (C═O amide), 1736 (CO, ester).^{1}H NMR (400 MHz, DMSO-d_6): δ 1.22 (t, J = 7.1 Hz, 3H, $COOCH_2CH_3$), 1.59 (m, 4H, $2CH_2$), 1.80 (m, 2H, CH_2), 2.83 (m, 2H, CH_2), 3.17 (m, 2H, CH_2), 3.91 (s, 2H, CH_2−S), 4.12 (q, J = 7.1 Hz, 2H, $COOCH_2CH_3$), 7.43 (m, 2H, Ar-H), 7.59 (m, 3H, Ar-H). ^{13}C NMR (100 MHz, DMSO-d_6): 14.65, 27.25, 27.47, 27.83, 29.38, 32.42, 34.83, 61.52, 119.58, 129.77, 130.49, 136.99, 158.78, 158.25, 160.09, 168.67.

*4.1.4. General Procedure for the Synthesis of 2-Alkylthio-3-(4-nitrophenyl)-6,7,8,9-hexahydro-3H-cyclohepta[4,5]-thieno[2,3-d]pyrimidin-4-(5H)-ones (**12**−**16**).* The appropriate alkyl halide (1.5 mmol) and a mixture of K_2CO_3 (0.18 g, 1 mmol) and compound **6** (0.37g, 1 mmol) in DMF (5 mL) were stirred for about 24 h at room temperature. The reaction mixture was poured onto iced water, the formed solid was filtrated and washed with water, and crystallization from ethanol was done.

*4.1.4.1. 2-Benzylthio-3-(4-nitrophenyl)-6,7,8,9-hexahydro-3H-cyclohepta[4,5]thieno[2,3-d]pyrimidin-4-(5H)-one (**12**).* Using benzyl chloride (0.19 g, 1.5 mmol) as the alkyl halide yielded a white solid; yield = 74%, melting point = 214−216 °C, IR (KBr, υ, cm^{-1}): 1350, 1513 (NO_2), 1686 (C═O), 1613 (C═C).^{1}H NMR (400 MHz, $CDCl_3$): δ 1.68 (m, 4H, $2CH_2$), 1.89 (m, 2H, CH_2), 2.88 (m, 2H, CH_2), 3.30 (m, 2H, CH_2), 4.37 (s, 2H, S-CH_2), 7.31 (m, 5H, Ar-H), 7.50 (d, 2H, Ar-H), 8.39 (d, 2H, Ar-H).

*4.1.4.2. 2-Methylthio-3-(4-nitrophenyl)-6,7,8,9-hexahydro-3H-cyclohepta[4,5]thieno[2,3-d]pyrimidin-4-(5H)-one (**13**).* Using methyl iodide (0.21 g, 1.5 mmol) as the alkyl halide yielded a white solid; yield = 77%, melting point = 223−225 °C. ^{1}H NMR (400 MHz, DMSO-d_6): δ 1.60 (m, 4H, $2CH_2$), 1.85 (m, 2H, CH_2), 2.82 (m, 2H, CH_2), 3.17 (m, 2H, CH_2), 3.85 (s, 3H, CH_3), 7.73 (d, J = 7.1 Hz, 2H, Ar-H). 8.36 (d, J = 7.1 Hz, 2H, Ar-H).

*4.1.4.3. 2-Cyclopentythio-3-(4-nitrophenyl)-6,7,8,9-hexahydro-3H-cyclohepta[4,5]thieno[2,3-d]pyrimidin-4-(5H)-one (**14**).* Using cyclopentyl bromide (0.15 g, 1.5 mmol) as the alkyl halide yielded a white solid; yield = 71%, melting point = 199−201 °C. ^{1}H NMR (400 MHz, $CDCl_3$): δ 1.45−2.12 (m, 14H, $7CH_2$), 2.85−3.18 (m, 4H, $2CH_2$), 3.93 (p, 1H, CH), 7.78 (d, J = 8.0 Hz, 2H, Ar-H), 8.40 (d, J = 8.0 Hz, 2H, Ar-H). ^{13}C NMR (100 MHz, DMSO-d_6): 21.13, 27.26, 27.52, 27.85, 29.40, 32.39, 79.35, 74.79, 119.77, 125.27, 131.82, 136.28, 137.06, 141.88, 148.79, 154.78, 158.09, 160.20.

*4.1.4.4. Ethyl 2-[3-(4-Nitrophenyl)-4-oxo-6,7,8,9-tetrahydro-3H-cyclohepta[4,5]thieno[2,3-d]pyrimidin-2-yl]-thioacetate (**15**).* Using ethyl chloroacetate (0.18 g, 1.5 mmol) as the alkyl halide yielded a white solid; yield = 88%, melting point = 213−215 °C, IR (KBr, υ, cm^{-1}): 1350, 1519 (NO_2), 1679 (C═O, amide), 1733 (CO, ester). ^{1}H NMR (400 MHz, DMSO-d_6): δ 1.22 (t, J = 7.1 Hz, 3H, CH_2CH_3), 1.60 (m, 4H, $2CH_2$), 1.81 (m, 2H, CH_2), 2.83 (m, 2H, CH_2), 3.17 (m, 2H, CH_2), 3.96 (s, 2H, CH_2-S), 4.13 (q, J = 7.1 Hz, 2H, CH_2CH_3), 7.83 (d, J = 8.8 Hz, 2H, Ar-H), 8.44 (d, J = 8.8 Hz, 2H, Ar-H).

*4.1.4.5. 3-(4-Nitrophenyl)-2-(prop-2-yn-1-ylthio)-6,7,8,9-tetrahydro-3H-cyclohepta[4,5]thieno[2,3-d]pyrimidin-4-(5H)-one (**16**).* Using propargyl bromide (0.17 g, 1.5 mmol) as the alkyl halide yielded a white solid; yield = 86%, melting point = 204−206 °C, IR (KBr, υ, cm^{-1}): 1350, 1519 (NO_2), 1682 (C═O), 3287 (CH SP). ^{1}H NMR (400 MHz, DMSO-d_6): δ 1.61(m, 4H, $2CH_2$), 1.81(m, 2H, CH_2), 2.86 (m, 2H, CH_2), 3.18 (m, 2H, CH_2), 3.22 (s, 1H, −CHS−), 3.95 (s, 1H, −CHS−), 7.82 (d, J = 8.7 Hz, 2H, Ar-H). 8.42 (d, J = 8.6 Hz, 2H, Ar-H). ^{13}C NMR (100 MHz, $CDCl_3$): 24.90, 27.27, 27.56, 27.87, 29.40, 32.41, 32.94, 45.60, 74.79, 119.51, 125.15, 131.77, 135.73, 137.01, 142.46, 148.59, 156.83, 158.21, 160.66.

*4.1.5. Synthesis of 2-(4-Oxo-3-phenyl-6,7,8,9-tetrahydro-3H-cyclohepta[4,5]thieno[2,3-d]pyrimidin-2-yl)-thioacetohydrazide (**17**).* A mixture of thioacetate **11** (0.41 g, 1 mmol) and hydrazine hydrate (0.10 g, 2 mmol) in absolute ethanol (4 mL) was stirred for 12 h at room temperature. When the TLC showed that the reaction was complete, filtration and purification using column chromatography (ethyl acetate/petroleum ether) gave a white solid, yield = 58%, melting point = 240−242 °C, IR (KBr, υ, cm^{-1}): 1514 (olefinic C═C), 1645 (CO, hydrazide), 1687 (C═O, amide), 3263, 3323 (NH_2). ^{1}H NMR (400 MHz, DMSO-d_6): δ 1.60 (m, 4H, $2CH_2$), 1.83 (m, 2H, CH_2), 2.84 (m, 2H, CH_2), 3.19 (m, 2H, CH_2), 3.78 (s, 2H, CH_2-S), 4.26 (s, 2H, NH_2; exchangeable with D_2O), 7.42 (m, 2H, Ar-H), 7.57 (m, 3H, Ar-H), 9.29 (s, 1H, NH; exchangeable with D_2O).

*4.1.6. General Procedure for the Synthesis of N′-Arylidene-2-[(4-oxo-3-phenyl-6,7,8,9-tetrahydro-3H-cyclohepta[4,5]thieno[2,3-d]pyrimidin-2-yl)thio]-acetohydrazide (**18**−**23**).* A hydrazide **17** suspension (0.43 g, 1 mmol) in absolute ethanol (3 mL) was added to the appropriate aromatic aldehyde (1 mmol). It was heated at 70 °C for 24 h. When the TLC showed that the reaction was complete, the separated solid was filtered and purified with silica gel chromatography (ethyl acetate/petroleum ether).

*4.1.6.1. Synthesis of N′-(4-Hydroxybenzylidene)-2-[(4-oxo-3-phenyl-6,7,8,9-tetrahydro-3H-cyclohepta[4,5]thieno[2,3-d]pyrimidin-2-yl)thio]acetohydrazid (**18**).* Using 4-hydroxybenzaldehyde (0.12 g) yielded a white solid; yield = 89%, melting point = 267−269 °C, IR (KBr, υ, cm^{-1}): 1607 (C═N), 1649 (C═O, hydrazide), 1688 (C═O, amide), 3067 (NH), 3261 (OH). ^{1}H NMR (400 MHz, DMSO-d_6): δ 1.55 (m, 4H, $2CH_2$), 1.84 (m, 2H, CH_2), 2.82 (m, 2H, CH_2), 3.18 (m, 2H, CH_2), 3.92 and 4.35 (s, 2H, S-CH_2, *trans*/*cis* conformers), 6.81 (m, 2H, Ar-H), 7.43 (m, 4H, Ar-H), 7.58 (m, 3H, Ar-H), 7.90 and 8.07 (s, 1H, N═CH, *trans*/*cis* conformers), 9.89 (s, 1H, NH, *trans*/*cis* conformers), 11.45 and 11.55 (s, 1H, OH). ^{13}C NMR (100 MHz, DMSO-d_6): 27.26, 27.49, 27.85, 29.37, 32.42, 34.80, 116.14, 119.50, 125.48, 129.04, 129.35, 129.83, 130.01, 135.67, 136.17, 136.97, 144.29, 157.30, 158.40, 159.70, 160.29, 168.60.

*4.1.6.2. Synthesis of N′-(3-Hydroxy-4-methoxybenzylidene)-2-[(4-oxo-3-phenyl-6,7,8,9-tetrahydro-3H-cyclohepta-[4,5]thieno[2,3-d]pyrimidin-2-yl)thio]aceto- hydrazide (**19**).* Using 3-hydroxy-4-methoxybenzaldehyde (0.15 g) yielded a white solid; yield = 87%, melting point = 247−249 °C, IR (KBr, υ, cm^{-1}): 1514 (olefinic C═C), 1585 (C═N), 1677 (C═O-amide), 3099 (NH), 3261 (OH). ^{1}H NMR (400 MHz, DMSO-d_6): δ 1.59 (m, 4H, $2CH_2$), 1.84 (m, 2H, CH_2), 2.82 (m, 2H, CH_2), 3.14 (m, 2H, CH_2), 3.80 (s, 3H, OCH_3), 3.91 and 4.35 (s, 2H, S-CH_2, *trans*/*cis* conformers), 6.98 (d, J = 7.3 Hz, 2H, Ar-H), 7.17 (s, 1H, Ar-H), 7.52 (m, 5H, Ar-H), 7.87 and 8.03 (s, 1H, N═CH, *trans*/*cis* conformers), 9.27 and 9.34 (s, 1H, NH, *trans*/*cis* conformers), 11.48 and 11.58 (s, 1H, OH, *trans*/*cis* conformers). ^{13}C NMR (100 MHz, DMSO-d_6): 27.26, 27.49, 27.85, 29.37, 32.42, 34.80, 116.14, 119.50, 125.48, 129.04, 129.35, 129.83, 130.01, 135.67, 136.17, 136.97, 144.29, 157.30, 158.40, 159.70, 160.29, 168.60.

https://doi.org/10.1021/acsomega.2c06078
ACS Omega 2022, 7, 45455−45468

*4.1.6.3. Synthesis of N′-(4-Fluorobenzylidene)-2-[(4-oxo-3-phenyl-6,7,8,9-tetrahydro-3H-cyclohepta[4,5]thieno[2,3-d]pyrimidin-2-yl)thio]acetohydrazid (**20**).* Using 4-flourobenzaldehyde (0.12 g) yielded a white solid; yield = 90%, melting point = 247−249 °C, IR (KBr, υ, cm^{-1}): 1514 (olefinic C═C), 1676 (C═O, amide), 3069 (NH). ^{1}H NMR (400 MHz, DMSO-d_6): δ 1.58 (m, 4H, $2CH_2$), 1.84 (m, 2H, CH_2), 2.81 (m, 2H, CH_2), 3.18 (m, 2H, CH_2), 3.95 and 4.37 (s, 2H, s, 2H, S-CH_2, *trans*/*cis* conformers), 7.28 (t, J = 5.8 Hz, 2H, Ar-H), 7.43 (t, J = 5.8 Hz, 2H, Ar-H) 7.58 (m, 2H, Ar-H), 7.73 (m, 3H, Ar-H), 8.01 and 8.19 (s, 1H, N═CH, *trans*/*cis* conformers), 11.66 and 11.77 (s, 1H, NH, *trans*/*cis* conformers).

*4.1.6.4. Synthesis of N′-(4-Nitrobenzylidene)-2-[(4-oxo-3-phenyl-6,7,8,9-tetrahydro-3H-cyclohepta[4,5]thieno[2,3-d]pyrimidin-2-yl)thio]acetohydrazid (**21**).* Using 4-nitrobenzaldehyde (0.15 g) yielded a gray solid; yield = 85%, melting point = 232−234 °C, IR (KBr, υ, cm^{-1}): 1340, 1515 (NO_2), 1591 (olefinic C═C), 1680 (C═O, amide), 3079 (NH). ^{1}H NMR (400 MHz, DMSO-d_6): δ 1.58 (m, 4H, $2CH_2$), 1.84 (m, 2H, CH_2), 2.81 (m, 2H, CH_2), 3.19 (m, 2H, CH_2), 3.99 and 4.41 (s, 2H, s, 2H, S-$\underline{CH_2}$, *trans*/*cis* conformers), 7.43 (d, J = 6.4 Hz, 2H, Ar-H) 7.58 (d, J = 6.6 Hz, 3H, Ar-H), 7.95 (m, 2H, Ar-H), 8.13 (s, 1H, N═CH), 8.28 (m, 2H, Ar-H), 11.97 (s, 1H, NH; D_2O exchangeable).

*4.1.6.5. Synthesis of N′-(3-Nitrobenzylidene)-2-[(4-oxo-3-phenyl-6,7,8,9-tetrahydro-3H-cyclohepta[4,5]thieno[2,3-d]pyrimidin-2-yl)thio]acetohydrazid (**22**).* Using 4-nitrobenzaldehyde (0.15 g, 1 mmol) yielded a gray solid; yield = 88%, melting point = 250−252 °C. ^{1}H NMR (400 MHz, DMSO-d_6): δ 1.58 (m, 4H, $2CH_2$), 1.84 (m, 2H, CH_2), 2.81 (m, 2H, CH_2), 3.18 (m, 2H, CH_2), 3.92 and 4.43 (s, 2H, s, 2H, S-CH_2, *trans*/*cis* conformers), 7.45 (m, 3H, Ar-H), 7.58 (d, J = 6.7 Hz, 2H, Ar-H) 7.74 (s, 1H, Ar-H), 8.21 (m, 3H, Ar-H), 8.51 and 8.53 (s, 1H, N═CH, *trans*/*cis* conformers), 11.90 and 12.03 (s, 1H, NH, *trans*/*cis* conformers). ^{13}C NMR (100 MHz, DMSO-d_6): 27.29, 27.47, 27.83, 29.15, 29.36, 32.39, 119.53, 129.80, 130.04, 130.09, 130.94, 133.49, 135.74, 136.98, 136.98, 141.75, 144.68, 157.30, 158.41, 159.11, 160.21, 169.37.

*4.1.6.6. Synthesis of N′-[4-(Dimethylamino)benzylidene]-2-[(4-oxo-3-phenyl-6,7,8,9-tetrahydro-3H-cyclohepta[4,5]thieno[2,3-d]pyrimidin-2-yl)thio]acetohydrazide (**23**).* Using 4-dimethyl aminobenzaldehyde (0.15 g, 1 mmol) yielded a white solid; yield = 86%, melting point = 229−231 °C, IR (KBr, υ, cm^{-1}): 1513 (olefinic C═C), 1606 ($\underline{CO}$−hydrazide), 1677 (C═O, amide), 3083 (NH). ^{1}H NMR (400 MHz, DMSO-d_6): δ 1.58 (m, 4H, $2CH_2$), 1.84 (m, 2H, CH_2), 2.81 (m, 2H, CH_2), 2.97 (s, 6H, $2CH_3$), 3.18 (m, 2H, CH_2), 3.92−4.34 (s, 2H, S-CH_2, *trans*/*cis* conformers), 6.72 (m, 2H, Ar-H), 7.43 (m, 3H, Ar-H) 7.55 (m, 4H, Ar-H), 7.87 and 8.03 (s, 1H, N=CH, *trans*/*cis* conformers), 11.36 and 11.44(s, 1H, NH, *trans*/*cis* conformers). ^{13}C NMR (100 MHz, DMSO-d_6): δ 18.65, 27.18, 29.30, 29.37, 32.42, 56.67, 112.18, 128.71, 129.60, 130.17, 136.87, 137.01, 145.14, 147.71, 152.38, 157.28, 159.98, 163.47, 166.41, 168.60.

*4.1.7. Synthesis of 2-{[2-(3,5-Dimethyl-1H-pyrazol-1-yl)-2-oxoethyl]thio}-3-phenyl-3,5,6,7,8,9-hexahydro-4H-cyclohepta[4,5]thieno[2,3-d]pyrimidin-4-one (**24**).* To hydrazide **17** (1.23 g, 3 mmol) in a minimum volume of hot anhydrous ethanol, acetylacetone (0.30 g, 3 mmol) was added. The reaction mixture was stirred for 3 days at room temperature, followed by evaporation of the solvent at room temperature. The obtained residue was collected and recrystallized from *n*-hexane to give a white solid; yield = 91%, melting point = 204−206 °C, IR (KBr, υ, cm^{-1}): 1512 (olefinic C═C), 1653 ($SCH_2\underline{CO}$−N), 1690 (C═O, amide). ^{1}H NMR (400 MHz, DMSO-d_6): δ 1.55 (m, 4H, $2CH_2$), 1.70 (S, 3H, CH_3), 1.85 (m, 2H, CH_2), 1.99 (S, 3H, CH_3), 2.84 (m, 2H, CH_2), 3.18 (m, 2H, CH_2), 4.14−4.27 (s, 2H, $\underline{CH_2}$-S), 6.39 (s, 1H, CH, pyrazole), 7.42 (m, 2H, Ar-H), 7.57 (m, 3H, Ar-H). ^{13}C NMR (100 MHz, DMSO-d_6): δ 16.35, 26.35, 27.26, 27.49, 27.85, 29.37, 32.41, 37.43, 52.51, 90.94, 119.48, 129.80, 130.03, 130.38, 135.65, 136.29, 136.29, 136.92, 155.95, 157.38, 158.38, 160.35, 164.32.

4.2. Biology. *4.2.1. In Vitro Cytotoxicity Screening.* Novel synthesized compounds were evaluated for their cytotoxic activities against the 60 cell lines at a single dose of 10 μM. The output from the single dose screening is represented as mean-graph charts of the percentage growth of survived cells and expressed as growth inhibition (GI %). Compounds with significant GI % are prepared at five different concentration levels and evaluated against the 60-cell panel.[26]

4.2.2. Human Dihydrofolate Reductase (hDHFR) Inhibition Assay. To verify the DHFR activity, an enzyme-linked immunosorbent assay (ELISA) was carried out. In this assay and at room temperature, addition of the standard and tested compounds to the plate wells that were coated with a specific antibody for *h*DHFR was done. The mean absorbance values of the standard solution and that of the tested compounds were detected. The absorbances and the standard concentrations were represented on the standard curve. In this curve, absorbances were represented on the Y-axis, and the concentrations were represented on the X-axis. The concentration/inhibition curve was utilized for detecting the IC_{50} values of the tested compounds.[27]

4.2.3. Analysis of Cell-Cycle Arrest. Measurement of the DNA content was dependent on flow cytometry analysis. The SNB-75 cell was treated with compound **20** in its exponential growth for 24 h. At the end of the incubation period, collection, centrifugation, and fixing of the cell with ice-cold ethanol were performed. The cell was treated with a buffer that contains 0.1% Triton X-100 and was PI-stained. A comparison with the control treated with DMSO was done, in which flow cytometry was used to measure the DNA content.

4.2.4. Apoptotic Assay. In the exponential growth phase, the SNB-75 cell was treated and incubated for 24 h with compound **20**. After that, the cells were suspended in a binding buffer, annexin V-FITC, to determine apoptosis and also suspended in PI to determine necrosis. To produce stability of the photo and enhance the signal of fluorescence, the annexin V-FITC conjugate was engineered. Flow cytometry was used to detect and analyze annexin V-FITC binding.[28]

4.2.5. Detection of Caspase-3 and Caspase-9 Protein Levels. The Invitrogen caspases-3 and -9 human kits (ELISA) were used to detect levels of human active caspases-3 and 9. To lyse the cell, an extraction buffer was added to the cells besides the tested compound. Incubation was carried out at room temperature, and washing of the wells was done 4 times. Incubation again at room temperature for 2 h was performed after active Invitrogen caspase-3 addition. Wells were precisely washed; the chromogen and horseradish peroxidase (HRP) solution (antirabbit IgG) were added and incubated for 30 min at room temperature. At 450 nm, the absorbance was measured.[24]

4.3. Molecular Modeling Methodology. A molecular docking analysis was performed using MOE software version

https://doi.org/10.1021/acsomega.2c06078
ACS Omega 2022, 7, 45455−45468

2014.09 in accordance with the standard MOE procedure.[29] The crystal structure of the DHFR interacting with its inhibitor MTX was obtained from the RSC Protein Data Bank (PDB code 1U72).[30,31] Construction of the three DHFR inhibitors (**20**, **22**, and **23**) was performed using the library of fragments in the MOE program. The "Amber force field" was used to minimize the energy of the inhibitors. The semiempirical mechanical calculation method "AM1" was adopted for assigning the partial atomic charges. The stochastic conformational search module was used to carry out the stochastic conformational search. All of these methods are performed using MOE program.

■ ASSOCIATED CONTENT

Supporting Information

The Supporting Information is available free of charge at https://pubs.acs.org/doi/10.1021/acsomega.2c06078.

Percent growth inhibition of selected compounds; ^{13}C NMR charts; and ^{1}H NMR charts (PDF)

■ AUTHOR INFORMATION

Corresponding Author

Walaa M. El Husseiny − *Department of Pharmaceutical Organic Chemistry, Faculty of Pharmacy, Mansoura University, Mansoura 35516, Egypt;* orcid.org/0000-0002-0261-8264; Email: walaaelhusseiny@yahoo.com

Authors

Ola A. Abdelaziz − *Department of Pharmaceutical Organic Chemistry, Faculty of Pharmacy, Mansoura University, Mansoura 35516, Egypt*

Khalid B. Selim − *Department of Pharmaceutical Organic Chemistry, Faculty of Pharmacy, Mansoura University, Mansoura 35516, Egypt*

Hassan M. Eisa − *Department of Pharmaceutical Organic Chemistry, Faculty of Pharmacy, Mansoura University, Mansoura 35516, Egypt*

Complete contact information is available at: https://pubs.acs.org/10.1021/acsomega.2c06078

Notes

The authors declare no competing financial interest.

■ REFERENCES

(1) Ng, H.-L.; Chen, S.; Chew, E.-H.; Chui, W.-K. Applying the designed multiple ligands approach to inhibit dihydrofolate reductase and thioredoxin reductase for anti-proliferative activity. *Eur. J. Med. Chem.* **2016**, *115*, 63−74.

(2) Raimondi, M. V.; Randazzo, O.; Franca, M. L.; Barone, G.; Vignoni, E.; Rossi, D.; Collina, S. DHFR inhibitors: reading the past for discovering novel anticancer agents. *Molecules* **2019**, *24*, 1140.

(3) Zhang, X.; Zhou, X.; Kisliuk, R. L.; Piraino, J.; Cody, V.; Gangjee, A. Design, synthesis, biological evaluation and X-ray crystal structure of novel classical 6,5,6-tricyclic benzo [4,5] thieno [2,3-*d*] pyrimidines as dual thymidylate synthase and dihydrofolate reductase inhibitors. *Bioorg. Med. Chem.* **2011**, *19*, 3585−3594.

(4) Yang, C.-R.; Peng, B.; Cao, S. L.; et al. Synthesis, cytotoxic evaluation and target identification of thieno [2,3-*d*] pyrimidine derivatives with a dithiocarbamate side chain at C2 position. *Eur. J. Med. Chem.* **2018**, *154*, 324−340.

(5) Gangjee, A.; Qiu, Y.; Li, W.; Kisliuk, R. L. Potent dual thymidylate synthase and dihydrofolate reductase inhibitors: classical and nonclassical 2-amino-4-oxo-5-arylthio-substituted-6-methylthieno [2,3-*d*] pyrimidine antifolates. *J. Med. Chem.* **2008**, *51*, 5789−5797.

(6) Gangjee, A.; Li, W.; Kisliuk, R. L.; Cody, V.; Pace, J.; Piraino, J.; Makin, J. Design, synthesis, and X-ray crystal structure of classical and nonclassical 2-amino-4-oxo-5-substituted-6-ethylthieno [2,3-*d*] pyrimidines as dual thymidylate synthase and dihydrofolate reductase inhibitors and as potential antitumor agents. *J. Med. Chem.* **2009**, *52*, 4892−4902.

(7) Sharaky, M.; Kamel, M.; Aziz, M. A.; Omran, M.; Rageh, M. M.; Abouzid, K. A. M.; Shoumana, S. A. Design, synthesis and biological evaluation of a new thieno [2,3-*d*] pyrimidine-based urea derivative with potential antitumor activity against tamoxifen sensitive and resistant breast cancer cell lines. *J. Enzyme Inhib. Med. Chem.* **2020**, *35*, 1641−1656.

(8) Deng, Y.; Zhou, X.; Desmoulin, S. K.; Wu, J.; Cherian, Ch.; Hou, Z.; Matherly, L. H.; Gangjee, A. Synthesis and biological activity of a novel series of 6-substituted thieno [2,3-*d*] pyrimidine antifolate inhibitors of purine biosynthesis with selectivity for high transporter for cellular entry. *J. Med. Chem.* **2009**, *52*, 2940−2951.

(9) Puterová, Z.; Krutošíková, A.; Gewald, D. V. Gewald reaction: synthesis, properties and applications of substituted 2-amino-thiophenes. *Arkivoc* **2010**, *2010*, 209−246.

(10) Gineinah, M. M.; Nasr, M. N. A.; Badr, S. M. I.; El-Husseiny, W. M. Synthesis and antitumor activity of new pyrido [2,3-*d*] pyrimidine derivatives. *Med. Chem. Res.* **2013**, *22*, 3943−3952.

(11) Wutticharoenwong, K.; Soucek, M. D. Influence of the Thiol Structure on the Kinetics of Thiol-ene Photopolymerization with Time-Resolved Infrared Spectroscopy. *Macromol. Mater. Eng.* **2008**, *293*, 45−56.

(12) Al-Amiery, A. A.; Musa, A. Y.; Kadhum, A. H.; Mohamad, A. The use of umbelliferone in the synthesis of new heterocyclic compounds. *Molecules* **2011**, *16*, 6833−6843.

(13) Socea, L. I.; et al. New Heterocyclic Compounds from 1,2,4-triazoles and 1,3,4-Oxadiazoles Class Containing 5H-dibenzo [a,d][7] Annulene Moiety. *Rev. Chem.* **2017**, *68*, 2761−2764.

(14) Al-Abdullah, E. S.; Asiri, H. H.; Lahsasni, S.; Habib, E. E.; Ibrahim, T. M.; El-Emam, A. Synthesis, antimicrobial, and anti-inflammatory activity, of novel S-substituted and N-substituted 5-(1-adamantyl)-1,2,4-triazole-3-thiols. *Drug Des. Dev. Ther.* **2014**, *8*, 505−518.

(15) Khurana, J. M.; Sahoo, P. K. Chemoselective alkylation of thiols: a detailed investigation of reactions of thiols with halides. *Synth. Commun.* **1992**, *22*, 1691−1702.

(16) Amr, A. E.-G. E.; Sabry, N. M.; Abdulla, M. M. Synthesis, reactions, and anti-inflammatory activity of heterocyclic systems fused to a thiophene moiety using citrazinic acid as synthon. *Monatsh. Chem.* **2007**, *138*, 699−707.

(17) El-Azab, A. S.; Abdel-Hamide, S. G.; Sayed-Ahmed, M. M.; Hassan, Gh. S.; El-Hadiyah, T. M.; Al-Shabanah, O. A.; Al-Deeb, O. A.; El-Subbagh, H. I. Novel 4 (3H)-quinazolinone analogs: synthesis and anticonvulsant activity. *Med. Chem. Res.*, **2013**, *22*, 2815−2827.

(18) Rando, D. G.; Sato, D. N.; Siqueira, L.; Malvezzi, A.; Leite, C. Q. F.; Amaral, A. T. d.; Ferreira, E. I.; Tavares, L. C. Potential tuberculostatic agents. Topliss application on benzoic acid [(5-nitro-thiophen-2-yl)-methylene]hydrazide series. *Bioorg. Med. Chem.* **2002**, *10*, 557−560.

(19) Zerov, A. V.; Krupenya, T. S.; Petrov, A. A.; Yakimovich, S. I. Reaction of trifluoromethyl-containing 1,3-dicarbonyl compounds with bis-hydrazides. *Russ. J. Org. Chem.* **2016**, *52*, 312−318.

(20) Grever, M. R.; Schepartz, S. A.; Chabner, B. A. The National Cancer Institute: cancer drug discovery and development program. *Semin. Oncol.* **1992**, *19*, 622−638.

(21) Boyd, M. R.; Paull, K. D. Some practical considerations and applications of the National Cancer Institute in vitro anticancer drug discovery screen. *Drug Dev. Res.* **1995**, *34*, 91−109.

(22) Al-Rashood, S. T.; Aboldahab, I. A.; Nagi, M. N.; Abouzeid, L. A.; Abdel-Aziz, A. A. M.; Abdel-Hamide, S. G.; Youssef, K. M.; Al-Obaid, A. M.; El-Subbagh, H. I. Synthesis, dihydrofolate reductase inhibition, antitumor testing, and molecular modeling study of some new 4 (3H)-quinazolinone analogs. *Bioorg. Med. Chem.* **2006**, *14*, 8608−8621.

(23) Fustero, S.; Sánchez, M.; Barrio, P.; Simón, A. A fruitful decade for the synthesis of pyrazoles. *Chem. Rev.* **2011**, *111*, 6984−7034.
(24) Scudiero, D. A.; Shoemaker, R. H.; Paull, K. D.; Monks, A.; Tierney, S.; Nofziger, T. H.; Currens, M. J.; Seniff, D. M.; Boyd, R. Evaluation of a soluble tetrazolium/formazan assay for cell growth and drug sensitivity in culture using human and other tumor cell lines. *Cancer Res.* **1988**, *48*, 4827−4833.
(25) Kathiravan, M. K.; Shishoo, C. J.; Chitre, T. S.; Mahadik, K. R.; Jain, K. S. Efficient Synthesis of Substituted 2-Amino-3-carbethoxythiophenes. *Synth. Commun.* **2007**, *37*, 4273−4279.
(26) Hassan, G. S.; El-Messery, S. M.; Al-Omary, F. A. M.; El-Subbagh, H. I. Substituted thiazoles VII. Synthesis and antitumor activity of certain 2-(substituted amino)-4-phenyl-1,3-thiazole analogs. *Bioorg. Med. Chem. Lett.* **2012**, *22*, 6318−6323.
(27) Priola, J. J.; Calzadilla, N.; Baumann, M.; Borth, N.; Tate, C. G.; Betenbaugh, M. J. High-throughput screening and selection of mammalian cells for enhanced protein production. *Biotechnol. J.* **2016**, *11*, 853−865.
(28) Ou, J.; Yu, Z.; Qiu, M.; et al. Knockdown of VEGFR2 inhibits proliferation and induces apoptosis in hemangioma-derived endothelial cells. *Eur. J. Histochem.* **2014**, *58*, No. 2263.
(29) Tran, T.-S.; Le, M.-T.; Tran, T.-D.; Tran, T.-H.; Thai, K.-M. Design of Curcumin and Flavonoid Derivatives with Acetylcholinesterase and Beta-Secretase Inhibitory Activities Using in Silico Approaches. *Molecules* **2020**, *25*, 3644.
(30) Abdelaziz, O. A.; El Husseiny, W. M.; Selim, K. B.; Eisa, H. M. Dihydrofolate reductase inhibition effect of 5-substituted pyrido [2,3-*d*] pyrimidines: Synthesis, antitumor activity and molecular modeling study. *Bioorg. Chem.* **2019**, *90*, No. 103076.
(31) Li, H.; Chen, S.; Chew, E.-H.; Chui, W.-K.; et al. Inhibitors of dihydrofolate reductase as antitumor agents: design, synthesis and biological evaluation of a series of novel nonclassical 6-substituted pyrido [2,3-*d*] pyrimidines with a three-to five-carbon bridge. *Bioorg. Med. Chem.* **2018**, *26*, 2674−2685.

https://doi.org/10.1021/acsomega.2c06078
ACS Omega 2022, 7, 45455−45468